

HIGH DUTY CYCLE SONAR TRACKING PERFORMANCE AS A FUNCTION OF COHERENT PROCESSING INTERVAL FOR LCAS'15 DATA

D. J. Grimmett^a, J. J. Itschner^a, D. A. Abraham^b, L. Mazutti^a

^aNIWC Pacific, 53560 Hull Street, San Diego, CA, 92131, grimmett@spawar.navy.mil

^bCausaSci LLC, P.O. Box 627, Ellicott City, MD 21041, UA, abraham@ieee.org

Abstract: *High Duty Cycle (HDC) sonar transmits with nearly 100% duty cycle. For LFM waveforms, this yields very large time-bandwidth products, with signal bandwidth swept over the entire transmission's ping repetition interval (PRI). In receive data processing, the PRI may be split up into shorter coherent processing intervals (CPIs), providing multiple detection opportunities per PRI. The potential advantage is an increased number of near continuous detection opportunities, leading to improved target localization, tracking, and classification, due to there being less time lapse between measurement scans. The corresponding disadvantage is that probability of detection and ranging accuracy may be lower per individual CPI detection opportunity. The choice of CPI for HDC sonar will influence detection and tracking performance.*

In this paper, the choice of CPI is evaluated using sonar data collected during the Littoral Continuous Active Sonar 2015 (LCAS'15) sea trial for a non-maneuvering surrogate target. A processing chain, including target tracker, is used to evaluate performance as a function of CPI. Typical track initiation algorithms (TIA) require setting parameters like SNR threshold and an M-of-N observation sequence to control the false track rates typical of clutter-rich environments. Previous analysis has been performed with fixed tracker parameters across different CPI settings, but here, we follow a more fair and operationally relevant comparison approach by specifying constant operationally relevant parameters for all cases, and by optimizing the tracker initiation M-of-N parameters for each individual case. Processing metrics such as probability of detection, and false alarm rate, as well as tracking metrics such as track-hold time, false track rate, and localization accuracy are reported. The relative advantages and disadvantages of reducing CPI are analyzed and explained for this dataset using these metrics at the output of a tracker.

Keywords: *Continuous Active Sonar, Tracking, Bandwidth, Sonar, High Duty Cycle*

1. INTRODUCTION

Recently, there has been emerging interest in the concept of High Duty Cycle (HDC) Sonar. Unlike Pulsed Active Sonar (PAS), which listens for echoes in between short transmission bursts, HDC sonar attempts to detect echoes amidst the continual interference from source(s) transmitting with nearly 100% duty cycle. Like PAS systems, HDC sonar systems may employ a variety of signal types. In this paper, we focus on the evaluation of continuous-time linear frequency modulated (CTLFM) waveforms for run E14 of the Littoral Continuous Active Sonar 2015 (LCAS'15) seatrial. HDC sonar offers a new parameter for the receiver signal processing chain: the coherent processing interval (CPI), which also corresponds to an equivalent processing sub-bandwidth of the LFM sweeps. The performance of HDC sonar is assessed as a function of the various user-selected processing intervals/sub-bandwidths, at the output of a target tracker. Previous efforts [1] compared performance using fixed tracker parameters, like SNR thresholds and track initiation logic. In this paper, we make comparisons by using optimum values for the track initiation algorithm (TIA) per CPI case, and tuning the tracker SNR threshold to achieve a constant false track rate at the output of the tracker. Various metrics are computed and compared at the input and output of the tracker.

HDC processing is discussed in Section 2. Section 3 describes the LCAS'15 experiment. Section 4 discusses the processing method and section 5 shows results at the tracker output. Section 6 provides a summary and conclusions.

2. HIGH DUTY CYCLE PROCESSING

Both PAS and HDC waveform signals repeat with a cycle time, referred to as the ping repetition interval (T_{pri}). T_{pri} defines the maximum range at which targets are detectable without becoming obscured by or ambiguously associated with acoustic energy from previous waveform cycles. For the HDC LFM waveform, the signal sweeps across the entire available bandwidth over the duration of the T_{pri} . This enables very large time-bandwidth (TB) products: an order of magnitude or more than is typically available with a corresponding PAS waveform with the same T_{pri} . Theory suggests that increasing the time-bandwidth (TB) product in processing will improve resolution in the time and/or Doppler dimensions and thereby increase the SNR in reverberation and/or noise-limited conditions, respectively. This is done by reducing the acoustic background, either by increasing the signal duration (to reduce ambient noise) or by increasing the signal bandwidth (to reduce reverberation), or both, while leaving the signal level un-diminished. However, in practice, achieving such theoretical gains is not entirely realizable due to environmental multipath spreading (energy splitting loss), echo Doppler shift and echo distributions of extended (non-point) targets [2,3].

Alternatively, one may choose to successively process multiple smaller TB segments of the entire waveform cycle. In this case, the individual echo SNRs may be smaller, but it offers many more opportunities to detect with rapid update rate, potentially providing good performance at the output of a target tracker. HDC sonar offers this new processing parameter (not available with PAS), specified as the coherent processing interval/time (CPI), and denoted hereafter as T_p . For LFM signals, T_p corresponds to a sub-bandwidth, B_p ; these may be chosen to tune the performance of the sonar. T_p can be chosen within the bounds of: $0 < T_p \leq T_{pri}$, (corresponding to $0 < B_p < B$). The choice will be a trade-off between how much TB to use for echo SNR gain vs. the desired number of detection opportunities available within a single T_{pri} . Fig. 1 (left) shows an example of the HDC processing interval. A common processing approach is to set up a bank of matched filters; one matched filter for each of the

selected sub-bands within a single cycle of the HDC LFM waveform. The sub-bands may be overlapped (in time/bandwidth) by about 50%, further increasing the number of detection scan opportunities, while maintaining measurements independence. Achieving more detection opportunities with a higher update rate can provide improvements in cumulative probability of detection, target initiation and holding, and target localization [4].

3. LCAS'15 EXPERIMENT

The LCAS'15 sea trial was conducted in September 2015, in shallow waters off the coast of La Spezia, Italy, in conjunction with an international research project with the Centre for Maritime Research and Experimentation (CMRE). Water depths ranged from 100-200m and reverberation-limited conditions were predominant. The research vessel R.V. Alliance towed an acoustic source capable of PAS and HDC transmissions over the frequency band of 1800-3400Hz. It also towed a monostatic triplet hydrophone receiver array. The R.V. Leonardo ship towed an echo repeater (E/R) system, which repeated the received HDC signals as a surrogate target.

The right hand image of Fig. 1 shows the geometry for run E14, which is analysed in this paper. The R.V. Alliance track is shown with heading of 122°T and speed of 3.5 kts, with the sonar source & receiver deployed at 50 meters depth. The E/R track is shown, traveling with heading 145°T at 3.2 kts. The run was designed to have the E/R at nearly constant bearing (63° T) relative to the source during the entire 1.3 hour run, with a target range-rate of -0.63 m/s (-1.2 kts). The transmitted signal was an LFM upswEEP from 1800-2600Hz ($B=800\text{Hz}$) over 20 seconds, and repeating every 20 seconds ($T_{pri}=20\text{s}$). The E/R has a selectable target strength (TS), which is the amount of amplification that is applied to the repeated signal. For this data, the TS was set to 17 dB. The FORA receive array is a triplet array, which provides port/starboard discrimination of received acoustic energy. The received hydrophone data were beamformed by an on-board processing system in real-time.

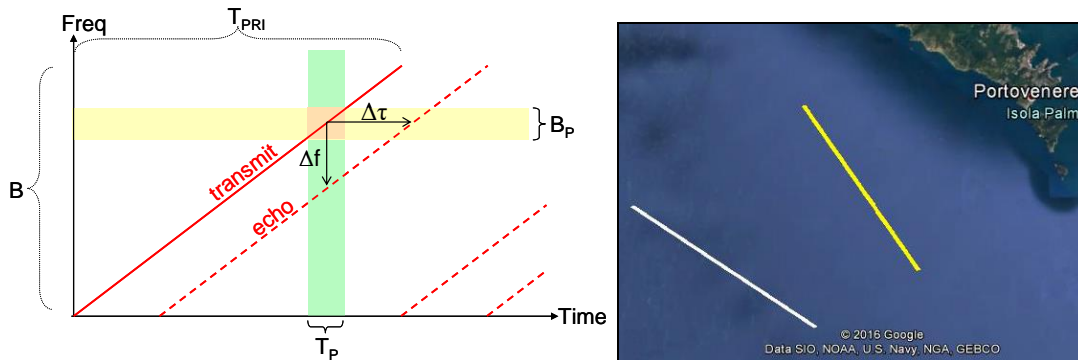


Fig. 1: Left-- Depiction of processing interval (green) and corresponding sub-band (yellow) for a continuous-time LFM signal in time and frequency. Right-- Geometry for run E14 of the LCAS'15 seatrial; Alliance (white) and E/R (yellow) tracks.

4. PROCESSING METHOD

HDC processing was accomplished using a bank of matched filters. The members of the replica bank correspond to a set of selected processing sub-bands, each with a bandwidth B_p at stepped-up center-frequencies to cover the total available signal bandwidth (B). The corresponding duration of each of the matched filter replicas is the processing time, T_p . In this paper, we evaluated the choice of T_p and B_p as a parameter, for the cases shown in Table 1. Also, the sub-bands were overlapped by about 50% in frequency (and equivalently

in time) to increase the detection scan rate, while still maintaining sample independence. The overlapping was not possible in the case of $T_p=20$ s, because the sub-band cannot cross the T_{pri} boundary.

The matched filtering is applied to each of the processed beams, and the outputs of the replica bank are time-aligned to create a multi-scan detection image with echo time-delay forming the x-axis and scan time the y-axis. An example output is shown in Fig. 2 (left) for the single beam pointed at the target, where the direct blasts are clearly seen near zero seconds time delay. The target echoes are seen with decreasing time delays from 10-6 s, over the duration of the run. Each matched filtered beam of the data was processed with a one-dimensional split-window normalizer in time, with guard and noise bands of 0.2 seconds length. Detection contacts are extracted from the data by clustering any time-contiguous data exceeding a threshold of 10 dB, and with at least one excursion above a higher threshold of 12 dB. Temporal detection clusters from adjacent beams were clustered if their time-extents overlap. The resulting information extracted from the detection clusters contain the arrival time and beam angle of the echo peak, time- and beam-extents of the detection cluster, and peak signal-to-noise ratio (SNR). Fig. 2 (right) shows extracted detection contacts for all beams. Using truth reconstruction, we determine which of the contacts that are associated to the target and tag them, enabling the computation of various performance metrics.

	Case 1	Case 2	Case 3	Case 4	Case 5	Case 6	Case 7
T_p (sec)	1.25	2.5	3.33	5	6.67	10	20
B_p (Hz)	50	100	133	200	267	400	800
Overlap (%)	50	50	50	50	50	50	0
$\#scans/T_{pri}$	31	15	11	7	5	3	1
N (scans in T_d)	95	47	35	23	17	11	3
K (scans)	95	47	35	23	17	11	3
M (scans)	32	21	18	13	11	8	2
h (dB)	14.13	15.15	15.3	15.7	15.5	15.6	19.25

Table 1: Test case processing intervals/sub-bands and tracker parameters.

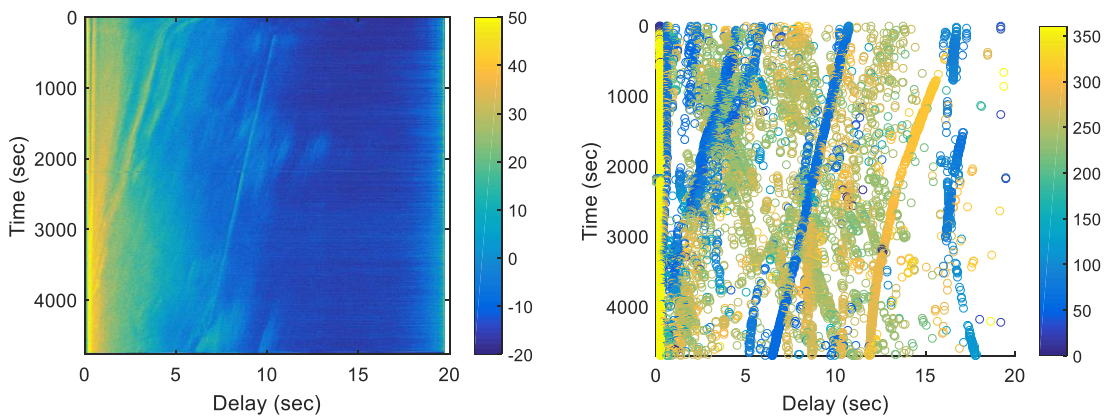


Fig. 2: Left-- Example HDC processing output for the target-pointing beam ($T_p=3.33$), output level in dB (in color) vs. scan-time vs. echo delay time. Right-- Example of extracted detection contacts above 15.5 dB, bearing (in color).

The processing was performed for each of the cases listed in Table 1, producing sets of detection contacts, per scan. A statistical analysis of the detection contacts for this data for different T_p cases has been done previously [1]. This showed that mean signal-to-noise ratio values increase somewhat with increasing T_p , but not to the extent predicted by theory. This is due the limitations in maintaining signal coherence in the acoustic channel due to time spreading/multipath [2,3].

5. TRACKING COMPARISONS

After the detection contacts were formed, they were input into a kinematic multi-target tracker [5]. We employ a simple but common track initiation algorithm (TIA). Tracks are confirmed by successful kinematic association of M detections above the tracker threshold h , within N sequential scans of the input data. Tracks are terminated after K consecutive scans where association was not successfully made.

In a previous analysis, comparative tracker performance (as a function of T_p) was obtained [1], however, it used fixed track initiation parameters (M , N , K , and h) for all cases. This may not be the most appropriate comparison method. In this paper, we choose to evaluate tracker performance using a different methodology which is better tied to operational requirements as follows: 1) we specify a constant, fixed time for track initiation, T_d , applicable to all cases, which results in a different N for each case, 2) we use a method [6,7] to determine an optimum setting of M , given N , for each case independently, and, 3) we specify a constant output false track rate (FTR) for all cases using the given M and N , and achieve it by adjusting the tracker input threshold h . For this study, we have chosen a track initiation time of $T_d=60$ s (three times the T_{pri}). From this operational specification, the N values are derived consistent with 50% overlapping for each case. To simplify analysis, we have chosen the track kill parameter K to be equal to N . Optimum values of M were obtained from the method in [7], and the required levels of h were ascertained from iterations of tracker runs to achieve a constant $FTR \approx 22$ tracks/hr (which is ~ 30 tracks for the run duration), using those M and N values. All final parameters used for the tracking comparison are summarized in Table 1, and the results will now be presented, using various standard tracker metrics [8].

Fig. 3 (top left) shows the tracker input FAR (for contacts which are not tagged as originating from the target and above h), which is seen to increase exponentially with decreasing T_p , due to the increases in the number of detection scans. Also shown is the tracker output FTR , which does not include any of the “true” target track segments (identified by having a majority of their tracker updates being supplied by true target-tagged contacts). It is seen that the tracker achieves FTR s close to the specified 22/hr for all the T_p cases.

Fig. 3 (top right) shows the tracker input probability of detection (PD) as a function of T_p for the target tagged contacts above h . Input PD is computed as the ratio of the number scans detecting the target to the total number of scans. To better assess the limits of performance, the target-tagged contact $SNRs$ were decremented by various amounts in post analysis and the tracker was re-run. This enables extension of comparisons to more challenging detection conditions not present in this data. The decrement values were 0, -2, -4, -6, -8, and -10 dB. The figure shows that better input PD is obtained around $T_p=5-10$ s, with it dropping at lower and higher T_p values. As the decrementing is applied, the input PD drops as expected until we reach a point where very few detections will be available for tracking the target.

Fig. 3 (bottom left) shows the PD at the output of the tracker. This is computed as the ratio of the number of scans contributing to true target tracks (including coasts) divided by the total number of scans. It may be thought of as the percentage of track holding time. The results show an expected drop in output PD as the target-contacts are decremented. The data show that PD is somewhat flat across many values of T_p , except at the lowest T_p case (1.25s) where

it is better, and at the highest T_p case (20s) where it is worse. The tracker appears to better improve PD (from input to output) for the lower T_p cases.

The tracker localization performance can be characterized by the mean track estimation error (estimated values versus true values) and by the area-of-uncertainty (AOU) within which the target exists with a certain probability. To quantify the AOU over the scenario duration and enable comparison between different contacts sets, we computed the mean of the cumulative sum of target track AOU over time, with a 99% probability of target containment. The mean localization error and AOU calculations are shown in Fig. 3 (bottom right), for the case without SNR decrementing. It is seen that there is a clear trend that both localization and localization uncertainty performance is greatly improved with shorter T_p .

Fig. 4 shows the output plots of the tracker for each T_p case, where target SNRs were decremented by 4 dB. We see an equivalent number of approximately 22 false tracks per hour in each case, consistent with our operational specification. The true target tracking performance degrades with increased T_p , by the decrease in the percentage of track holding. In addition, there is an increase in tracker fragmentation resulting in multiple tracker output segments for the target, from no fragmentations for $T_p=1.25$ s to 4 fragmentations for $T_p=20$ s. Here the track segments are killed and sometimes reinitiated and this is another undesirable tracker behaviour to consider for performance. The false tracks show some consistency across cases, indicating that they are commonly viewing acoustic energy from clutter objects and/or environmental features producing it. False track's lengths tend to be longer with the lower T_p cases, consistent with the larger values of N and K used.

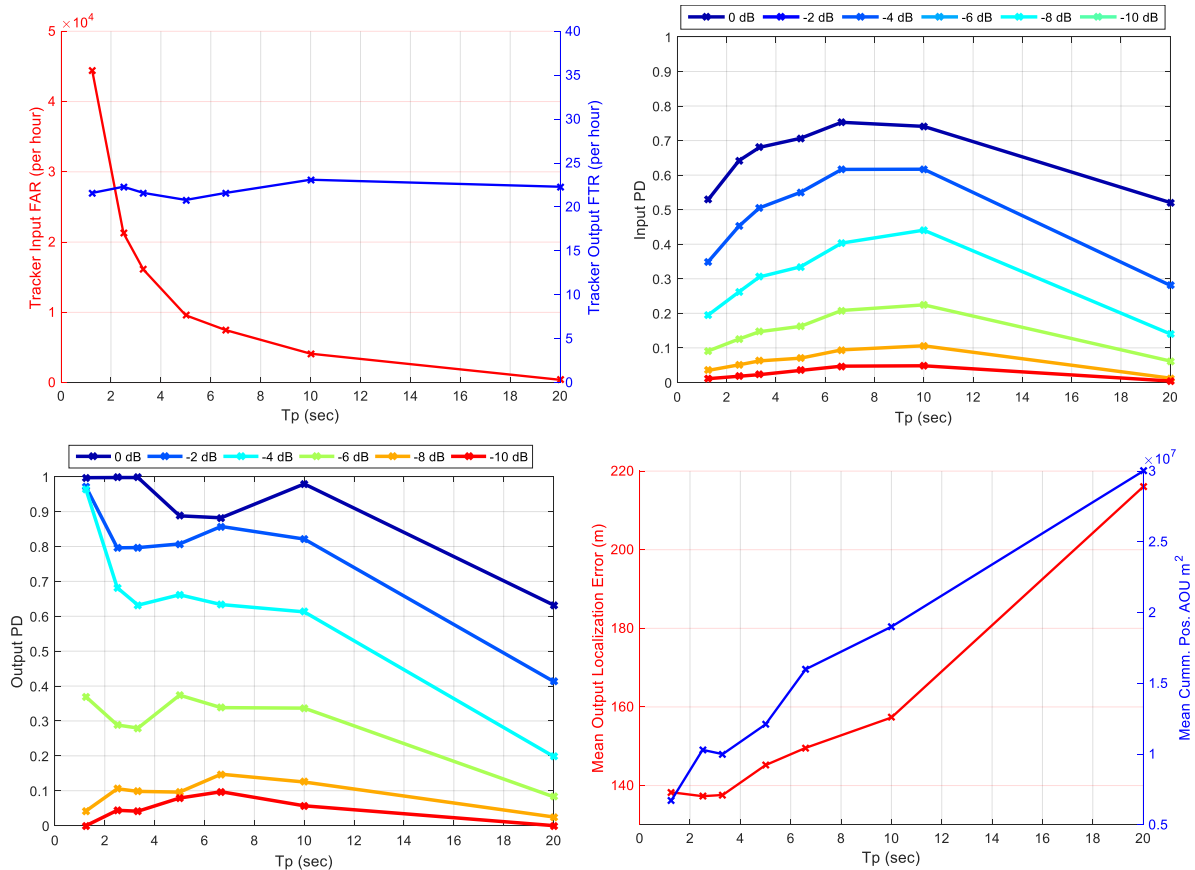


Fig. 3: Tracker metrics as a function of T_p . Top Left-- Tracker input false alarm rate (FAR) and tracker output false track rate (FTR) with no SNR decrement; Top Right-- tracker input probability of detection (PD) with various levels of decrementing; Bottom Left-- tracker output probability of detection with various levels of decrementing; Bottom Right-- tracker mean localization error and estimation uncertainty.

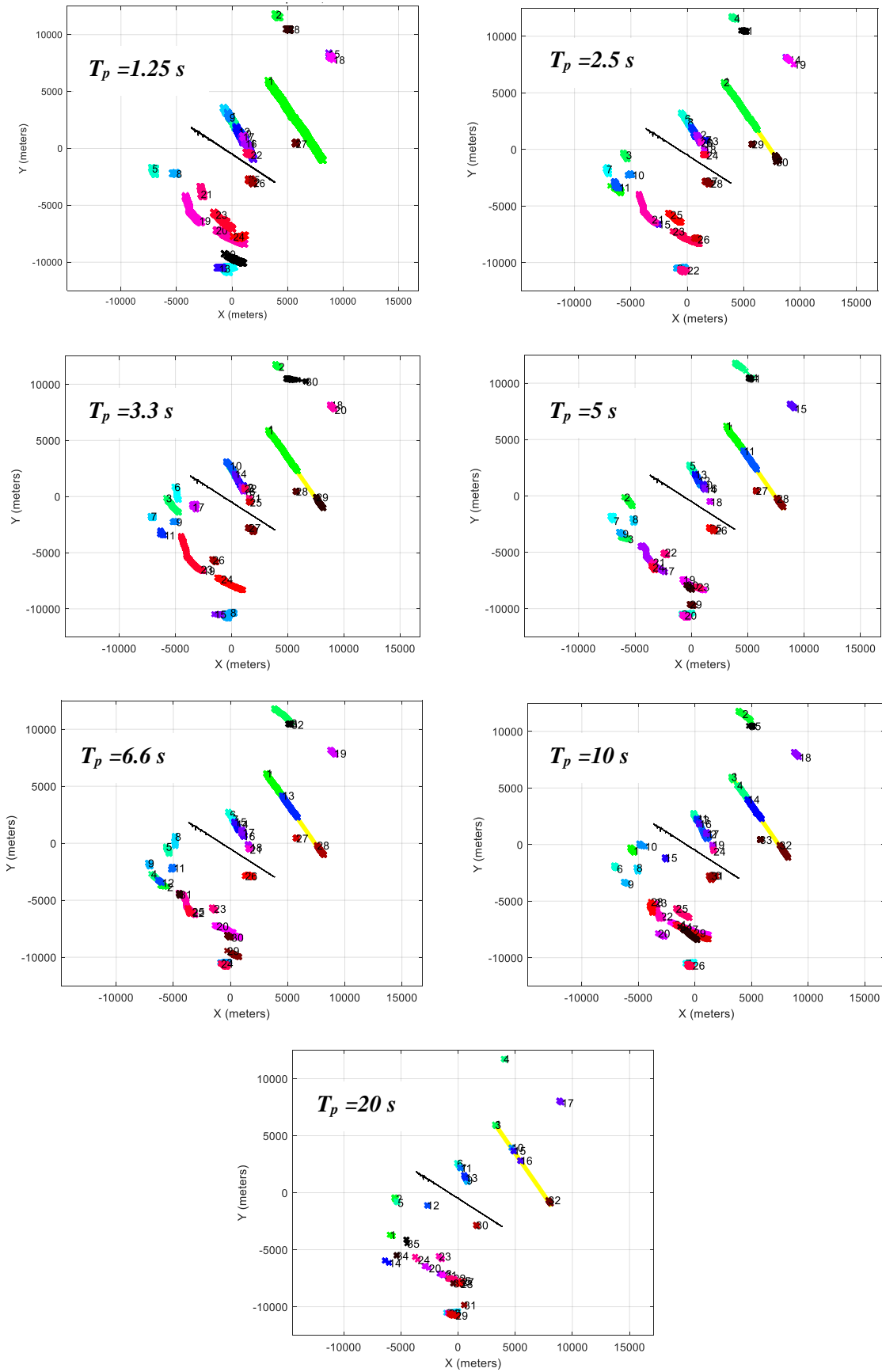


Fig. 4: Tracker output for the various T_p cases with ~ 30 output tracks; true target trajectory (yellow), ship trajectory (black), output tracks (numbered, with various colors).

6. SUMMARY AND CONCLUSIONS

The analysis of the LCAS'15 data offers insight into the tracking performance of HDC sonar as a function of a key new parameter: the HDC coherent processing interval, CPI (or T_p , or B_p). This parameter was investigated using a complete processing chain including kinematic tracker in order to evaluate processing chain end-to-end performance. The comparison approach was to specify the track initiation time and compare performance with constant output FTR , while optimizing the choice of M . The results show better tracking performance at lower values of T_p , in terms of target track holding, localization accuracy and localization uncertainty. The increased number of detection opportunities provided by shorter T_p offers improvement in localization. The tracker enhances the PD at lower T_p more than at high T_p . This comparison methodology may also be applied to evaluate how consistent performance is for different operational parameters (T_d and FTR).

7. ACKNOWLEDGEMENTS

We acknowledge the NATO CMRE LCAS Multinational Joint Research Project participants for their resources and support and in the planning, execution and analysis of this trial. Funding for this work was provided by ONR 321US.

REFERENCES

- [1] **D. Grimmert, R. Plate**, High Duty Cycle Sonar Performance as a Function of Processing Time-Bandwidth for LCAS'15 Data, Editor, in *Proc. of the 5th International Conference on Underwater Acoustics*, Skiathos, Greece, July 2019.
- [2] **R. Plate, D.J. Grimmert**, High Duty Cycle (HDC) Sonar Processing Interval and Bandwidth Effects for the TREX'13 Dataset, *Proc. of the MTS/IEEE Oceans'15 Conference*, volume (number), Genova, Italy, May, 2015.
- [3] **D. Grimmert, R. Plate**, Temporal and Doppler Coherence Limits for the Underwater Acoustic Channel during the LCAS'15 High Duty Cycle Sonar Experiment, *Proc. of the MTS/IEEE Oceans'16 Conference*, September, 2016, Monterey, CA.
- [4] **D. J. Grimmert**, Target AOU Growth Containment using LFM High Duty Cycle Sonar Editor, in *Proc. of the 2nd International Conference on Underwater Acoustics*, Rhodes, Greece, June, 2014.
- [5] **S. Coraluppi, D. Grimmert**, Multistatic Sonar Tracking, in *Proc. Of the SPIE Conference of Signal Processing, Sensor Fusion, and Target Recognition XII*, April 2003, Orlando, FL, USA.
- [6] **D. Abraham, D. Grimmert, J. Itschner**, Optimizing a Sliding M-OF-N Track Initializer in Clutter, Editor, in *Proc. of the 5th International Conference on Underwater Acoustics*, Skiathos, Greece, July 2019.
- [7] **D. Abraham**, Optimization of M-of-N in heavy-tailed noise. In *Proceedings of 2018 IEEE/MTS Oceans Conference*, Charleston, SC, 2018.
- [8] **S. Coraluppi, D. Grimmert, and P. de Theije**, Benchmark Evaluation of Multistatic Trackers, in *Proceedings of the 9th International Conference on Information Fusion*, July 2006, Florence, Italy.